THE JOURNAL OF PHYSICAL CHEMISTRY B

Article

pubs.acs.org/JPCB

Effect of Surface Energy on Carbon Dioxide Hydrate Formation

Junfang Zhang,[†,*] Mauricio Di Lorenzo,[†] and Zhejun Pan[‡]

[†]CSIRO CESRE, 26 Dick Perry Ave, WA 6151, Australia

[‡]CSIRO CESRE, Ian Wark Laboratory, Bayview Ave, Clayton, Vic 3168, Australia

ABSTRACT: In this work, the effect of the surface energy between the hydrate clusters and the aqueous phase on the hydrate formation of carbon dioxide was thoroughly investigated. Our results show that the threshold pressure for hydrate formation is less sensitive to the temperatures if the surface energy is not larger than 7 mJ/m^2. However, the threshold pressure is very sensitive to the temperatures and increases significantly with the surface energy if it is over 7, 9, and 10 mJ/m^2 for the temperatures of 279, 277.45, and 276 K, respectively. The value of the surface energy for the CO_2 hydrate/water system was determined as 9.3 mJ/m^2 by comparing our results with the experimental data for stable CO_2 hydrate formation at the temperature range of 277.45−278.85 K and at pressures of 55−165 bar. This value is very close to the recently reported value of 7.5 ± 1.4 mJ/m^2 from molecular simulation. A theoretical method was proposed for computing the induction time of hydrate formation adopting a composite of the time required for critical nuclei formation and their growth to a detectable size. By using this method, the surface energy was avoided in the induction time calculation and an average crystallite volume of 0.238 mm^3 at the induction time was derived based on the experimental data. It provides an approach for predicting the induction time for gas hydrate formation.

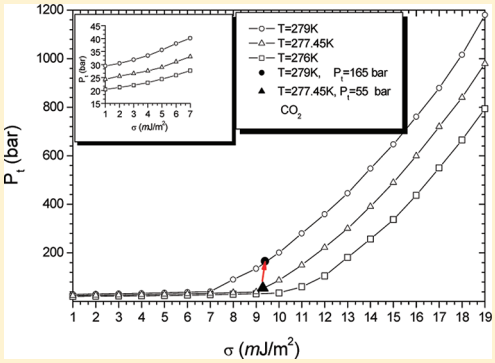

1. INTRODUCTION

Gas hydrates are a type of clathrate. Clathrates are complexes formed when guest molecules of one type are trapped inside a host lattice formed by another type of molecule.[1] The host lattice is the closest packing of polyhedral cagelike structures formed by hydrogen bonds between water molecules. The guest molecules are accommodated in the host lattice.[2,3] In fact, many different compounds can form clathrate hydrates. The different components typically give rise to one of three types of gas hydrate that differ in the crystal structure of the host lattice and hence in the number and size of the cages found in the lattice. The type of the gas hydrate depends primarily on the sizes and shapes of the guest molecule. The host lattices, which are less stable than ice, are stabilized by the van der Waals interaction between the guest and host molecules. Gas hydrates are formed at high pressure and low temperature. They are found in vast quantities in natural environments, such as permanently or seasonally frozen ground in polar regions, or marine sediment exposed to low-temperature and high-pressure environments. There is a growing research interest in gas hydrates due to the hazards they pose to oil and gas drilling and production operations.[4] The formation of gas hydrates can cause costly and hazardous blockage of natural gas pipelines.[5] The study on hydrate formation kinetics usually includes two areas. The first area deals with the primary nucleation process. The second concerns the process of crystal growth. Gas hydrate nucleation and growth have been investigated, with considerable working having been performed in recent years using a variety of experimental and modeling methods.[6−19] The rate at which hydrate nuclei form and grow is related to the thermodynamic driving force. The model of Englezos et al.[7,8] used the difference between the fugacity of the dissolved gas and the three-phase equilibrium fugacity as the driving force for particle growth. The model developed by Kashichiev and Firoozabadi[9−11] used the difference between the chemical potential of a hydrate building unit in the aqueous solution and in the hydrate crystal, also referred to as supersaturation, as the driving force. Supersaturation is defined as the difference between Gibbs free energy of a hydrate unit in the supersaturated aqueous phase and the hydrate phase. In these studies, the value of the surface energy between the hydrate clusters and the aqueous phase was assumed to be approximated by that of the surface energy between ice and liquid water.[20,21] Surface energy is difficult to measure but a very important and sensitive parameter influencing hydrate formation. It is also very crucial in the modeling of phase equilibrium. The lack of reliable values for hydrate−liquid interfacial tension has hindered the modeling studies of hydrate nucleation. Ben Clennell et al.[22] have used an interfacial tension of 27 mJ/m^2. Zhang et al.,[23] Klauda et al.,[24] and Henry et al.[25] used the hydrate−liquid interfacial tension of 26.7 mJ/m^2. Uchida et al.[26] measured the interfacial tensions of CH_4 hydrate−water, CO_2 hydrate−water, and C_3H_8 hydrate−water, which are 17 ± 3, 14 ± 3, and 25 ± 1 mJ/m^2, respectively. Anderson et al.[27] determined the interfacial tensions for ice−water, CH_4 hydrate−water, and CO_2

Received: March 6, 2012
Revised: May 11, 2012
Published: May 17, 2012

   dx.doi.org/10.1021/jp3021613 | J. Phys. Chem. B 2012, 116, 7296−7301

hydrate−water to be 32 ± 2, 32 ± 3, and 30 ± 3 mJ/m^2, respectively. However, Sakamaki et al.[28] have recently reported a value of 7.5 ± 1.4 mJ/m^2 for the hydrate−water interfacial tension.

In this work, the surface energy effect on CO_2 hydrate formation in aqueous solutions is investigated. The relationship between the threshold pressure for hydrate formation and the surface energy is determined by applying the kinetic model of Kashchiev et al.[9−11] and Anklam et al.[29] A method for computing the induction time of hydrate formation is proposed. By using this method, the induction time was theoretically predicted for CO_2 hydrate at temperatures of 276 and 279 K. The theoretical results for the induction time agree reasonably with the experimental data reported.[30]

2. MODELING DETAILS

Driving Force for Gas Hydrate. The driving force for new phase formation is the difference between the chemical potentials of the old and new phases and is defined for multicomponent system as

$$\Delta g = \sum_i n_i \Delta\mu_i \tag{1}$$

where n_i is the number of molecules of component i in repeated units of the newly created phase (here, the unit cell is chosen as the repeated unit), and $\Delta\mu_i$ is the driving force for component i. Anklam and Firoozabadi[29] have derived general expressions for the driving force per unit cell for forming a critical hydrate nucleus at a given temperature T and pressure P,

$$\Delta g = n_w\{\upsilon_w(P - P_e) - \upsilon_{hw}(P - P_e)\} + \sum_i n_i(T, P_e, y)kT\ln\frac{f_{gi}(T, P, y)}{f_{gi}(T, P_e, y)} \tag{2}$$

where, n_w is the number of water molecules in a unit cell, υ_{hw} is the molecular volume of water in the hydrate (the volume of hydrate unit cell divided by the number of water molecules in the unit cell), P_e is the equilibrium pressure and it was evaluated for every temperature, υ_w is molecular volume of water in solution, $n_i(T, P_e, y)$ is the number of gas molecule in a unit cell of hydrate, $f_{gi}(T, P, y)$ is the fugacity of species i in the gas phase. It is a function of temperature T, pressure P, and composition y. Eq 2 was derived under the following assumptions. The aqueous liquid and gas phases are in equilibrium so the chemical potential of gas in solution is the same as those in the gas phase. The mole fraction of water is very close to one and the activity coefficient of water can be approximated as one and the chemical potential of water is a function of T and P only. The volume of water molecule in solution and hydrate does not depend on the pressure. The number of water molecules in the hydrate unit cell is fixed for the given structure type and the driving force only involves the chemical potentials for species in the aqueous liquid and hydrate phases. The volume of the unit cell is independent of the composition of the hydrate. The fugacity coefficient can be calculated from the Soave−Redlich−Kwong equation of state.[31]

Nucleus Size. The general formulas for nucleus size n^* and nucleation work W^*, which are applicable to hydrate nucleation are expressed as.[9]

$$n^* = \frac{8c^3\upsilon_b^2\sigma^3}{27\Delta g^3} \tag{3}$$

$$W^* = \frac{4c^3\upsilon_b^2\sigma^3}{27\Delta g^2} \tag{4}$$

where c is a numerical shape factor, υ_b is the building unit volume (chosen as unit cell in this study), σ is surface energy, and Δg is the driving force calculated by eq 2.

Nucleation Rate. According to nucleation theory, in the case of stationary nucleation of multicomponent phase, the nucleation rate J is given by the general expression,[32]

$$J = A\exp\left(\frac{\Delta g}{kT}\right)\exp\left(-\frac{W^*}{kT}\right) = zf_e^*C_0\exp\left(\frac{\Delta g}{kT}\right)\exp\left(-\frac{W^*}{kT}\right) \tag{5}$$

where the kinetic factor A is defined as

$$A = zf_e^*C_0 \tag{6}$$

For hydrate nucleation in aqueous solutions, $C_0 = 1/\upsilon_w = 3 \times 10^{28}m^{-3}$. z is the so-called Zeldovich factor and is related to the nucleus size n^* and the nucleation work W^* by

$$z = \left(\frac{W^*}{3\pi kTn^{*2}}\right)^{1/2} \tag{7}$$

f^*_e depends on the specifics of the kinetics of attachment of hydrate building units to the surface of the hydrate nucleus. When this attachment is governed by volume diffusion of dissolved gas toward a homogeneously formed nucleus in isothermal regime, f^*_e has the form[32]

$$f_e^* = \varepsilon(4\pi c)^{1/2}\upsilon_b^{1/3}DC_en^{*1/3} \tag{8}$$

where ε is the sticking coefficient of hydrate building units to the nucleus surface, c is a numerical shape factor ($c = (36\pi)^{1/3}$ for spherical clusters), D is the diffusion coefficient of dissolved gas in the aqueous solution, C_e is the concentration of dissolved gas at phase equilibrium between hydrate and solution, and n^* is determined by eq 3. In this study, $\varepsilon = 1$, $c = (36\pi)^{1/3}$, $D = 0.001$ mm^2/s, $C_e = 0.03$nm^{-3}, and $\upsilon_b = 5.18$ nm^3 for structure II hydrate, and $\upsilon_b = 1.728$ nm^3 for a structure I hydrate.

Induction Time. The induction time is normally understood as the time needed to detect the appearance of the first hydrates from the solution. The experimentally determined value is affected by several parameters such as the initial supersaturation, temperature, agitation speed, and the presence of additives. It depends on the technique used to detect the formation of the new phase and hence is not a fundamental property of the system being studied. However, it is experimentally accessible and offers valuable information about the kinetics of hydrate nucleation and growth. Therefore, reliable methods for the determination of induction time periods are important. A turbidity measurement-based experimental method for the determination of the crystallization induction period has been used.[30,33] The induction time determined by turbidity measurement is a composite of the time required for critical nuclei formation and their growth to a detectable size. There are various definitions of the induction time.[32] A well-known definition is the one related to the temporal evolution of the volume of the new phase. Namely, the induction time, t_{ind}, is defined as the time needed for the formation of an a priori specified detectable volume, $V(t)$, of the new phase out of the total solution volume of V_s.

dx.doi.org/10.1021/jp3021613 | J. Phys. Chem. B 2012, 116, 7296−7301

According to this definition, the induction time will depend on the sensitivity of the technique chosen to detect the first hydrate appearance. Therefore, it is not easy to compare the theory with the experiment. To make a connection between nucleation theory and experimental investigation, a theoretical method for computing the induction time is proposed in the present work. The derivation of the volume of hydrate crystallized has been described in detail in other publication[11] and so we give here only a brief outline of the scheme employed for completeness of the derivation. Let $\alpha(t)$ be the ratio of the hydrate volume crystallized, $V(t)$, to the initial volume of the solution, V_s:

$$\alpha(t) = V(t)/V_s \tag{9}$$

Then the hydrate volume increment dV that is formed between time t' and $t' + dt'$, is

$$dV = V_c(t', t)j(t')V_s dt' \tag{10}$$

where $j(t')$ is the hydrate nucleation rate. For the steady-state nucleation rate, $j(t') = J$; $V_c(t',t)$ is the volume of any individual crystallite at time t, which depends only on the earlier moment t' $(0 \leq t' \leq t)$.

Limiting the analysis only to crystallites nucleated with negligibly small volume and growing in three dimensions, the individual crystallite volume $V_c(t',t)$ can be expressed as

$$V_c(t', t) = br^3(t', t) = b[\int_0^{t-t'} g(t'')dt'']^3 \tag{11}$$

where $r(t)$ is the crystallite radius, $g(t) \equiv dr(t)/dt$ is the crystallite growth rate, and b is a dimensionless shape factor. According to the power law of crystallite growth,

$$r(t) = (Gt)^m \tag{12}$$

where $m = {}^1/_2$ for growth by undisturbed volume diffusion of dissolved gas toward a spherical crystallite, and the crystallite growth constant G is expressed as

$$G = Q(e^{\Delta g/kT} - 1) \tag{13}$$

where the Δg-independent kinetic factor Q is given by

$$Q = 2\varepsilon\upsilon_b DC_e \tag{14}$$

Integrating eq 10, in view of eqs 11−14, and substituting the result into eq 9, the relationship between the induction time t_{ind} and the detectable hydrate fraction $\alpha(t_{ind})$ can be written as

$$\alpha(t_{ind}) = [bG^{3m}J/(1 + 3m)]t_{ind}^{1+3m} \tag{15}$$

Now, a quantity of average crystallite volume, $\bar{V}_c$, is introduced. At time t, the total number of the crystallites is

$$N_c = \int_0^{t_{ind}} JV_s dt = JV_s t_{ind} \tag{16}$$

Then

$$\alpha(t_{ind}) = \frac{\bar{V}_c N_c}{V_s} = \bar{V}_c J t_{ind} \tag{17}$$

Substituting eq 17 into eq 15, t_{ind} is expressed as

$$t_{ind} = (\bar{V}_c(1 + 3m)/b)^{1/3m} G^{-1} \tag{18}$$

Eq 18 is used to fit the induction time measured from experiments over a range of supersaturation values. The advantage of introducing eq 17 is that the J on both sides of eq 15 is canceled, which avoids the surface tension included in the expression of J in eq 5 through eq 4. Consequently, the induction times from the experiments can be fitted by only adjusting one parameter of $\bar{V}_c$.

3. KINETIC MODEL RESULTS AND DISCUSSION

In this section, we present the results obtained by applying the above-described kinetic model to the gas hydrate of CO_2. We show the surface energy dependence of the threshold pressure and the nucleation rate. Figure 1 shows the temperature and pressure dependence of the driving force for CO_2 hydrate at temperatures of 276 and 279 K. It is shown that the driving force increases with increasing pressure and decreasing temperature. Figure 2 displays the pressure and surface energy dependence of the homogeneously formed nucleus size n^* and nucleation work W^* for the CO_2 hydrate when Δg is varied isothermally at 276 K by changing pressure. The calculations are made according to eqs 3 and 4 with Δg from eq 2. The nucleus size and nucleation work are found to highly depend on the surface energy between hydrate and water and the pressure. It is observed that the lower value of the surface energy and higher pressure diminish both the nucleus size and the nucleation work. Low surface energy indeed implies a heterogeneous nucleation. As the surface energy between water and hydrate increases, the nucleus size and nucleation work will also increase. Kashchiev and Firoozabadi have demonstrated that heterogeneous nucleation of cap-shaped hydrate clusters on hydrate wetted solid surfaces in solution is thermodynamically favored over homogeneous nucleation.[10] For homogeneous nucleation of hydrate, a surface energy of 20 mJ/m^2 between water and ice was usually used for the surface energy between the hydrate clusters and the aqueous phase.[9−11] The surface energy between the hydrate and water is hard to be measured experimentally. Uchida et al.[26] estimated it by measuring the dissociation temperature for methane, carbon dioxide, and propane hydrate in different sizes of pores and fitting the experimental data to the Gibbs−Thomson equation with the surface energy as the fitting parameter. Jensen et al.[34] linearized the expression of the induction time based on crystallization theory[9] and fitted the experimentally obtained induction period to the model to determine the effective surface energy and kinetic constant. They used the ice−water surface energy of 20 mJ/m^2 as hydrate−water surface energy for homogeneous nucleation to obtain the contact angle for

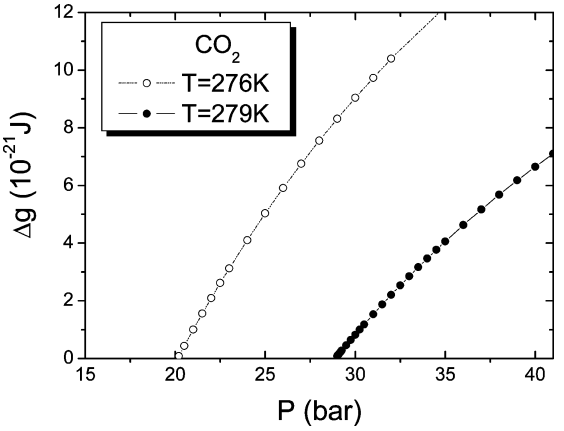

Figure 1. Comparison of driving forces for CO_2 hydrate at temperatures of 276 and 279 K.

dx.doi.org/10.1021/jp3021613 | J. Phys. Chem. B 2012, 116, 7296−7301

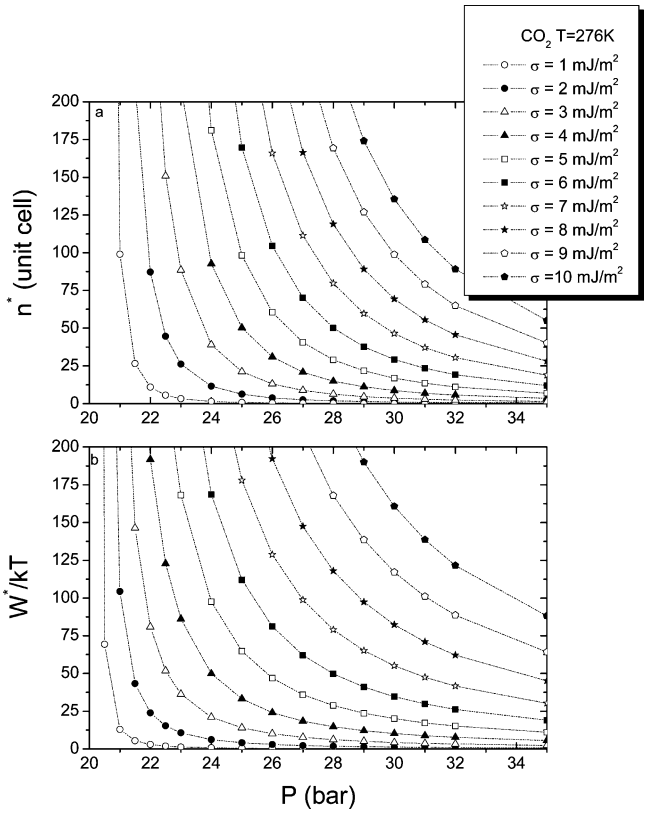

Figure 2. The pressure and surface energy dependence of (a) the nucleus size n^* and (b) nucleation work W^* for CO_2 hydrate at 276 K.

heterogeneous nucleation. Figure 3 depicts the curve of nucleation rate versus pressure with different surface energies specified (1−8 mJ/m^2) at temperatures of 276 K (part a of Figure 3) and 279 K (part b of Figure 3). As it is seen, the surface energy and pressure significantly affect the hydrate nucleation rate. As the surface energy increases and pressure reduces, the nucleation rate decreases. It should be noted that the equilibrium pressures (P_e) at 276 and 279 K are 20.13 and 28.89 bar, respectively. It is observed that below a threshold pressure, P_t, ($P_t > P_e$), nucleation in the solution is virtually arrested, for example, at T = 276 K, for σ = 8 mJ/m^2, no detectable nucleation occurs if pressure is below 29.67 bar, but, for σ = 3mJ/m^2, detectable homogeneous nucleation happens at pressure above 21.96 bar; At T = 279 K, for σ = 8 mJ/m^2, pressure should be larger than 45.00 bar in order to observe hydrate nucleation, but only 31.82 bar if σ is reduced to 3mJ/m^2. Similarly, in Figure 4, we show the nucleation rate vs pressure with different surface energies specified (9−20 mJ/m^2) for CO_2 hydrate at the two different temperatures of 276 and 279 K. The threshold pressure for the CO_2 hydrate formation as a function of the surface energy between the hydrate and aqueous solution is investigated. The results are shown in Figure 5 and tabulated in Table 1. The insert in Figure 5 shows the threshold pressure for the surface energies ranging from 1 to 7 mJ/m^2. Our results can be applied to heterogeneous nucleation (HEN), where an effective surface energy $\sigma_{ef} = \Psi\sigma$ is used and the factor Ψ is a number between 0 and 1. For homogeneous nucleation (HON), Ψ = 1 and $\sigma_{ef} = \sigma$. As it is seen, the threshold pressure increases significantly with the surface energy if the surface energy is over 7mJ/m^2 at 279 K, 9 mJ/m^2 at 277.45 K and 10 mJ/m^2 at 276 K. If the surface energy is not larger than 7 mJ/m^2, the threshold pressure is less sensitive to the temperature. In Figure 6, we show the experimental results for stable CO_2 hydrate formation at the temperature range of 277.45−278.85 K and the indicated pressures of 55−165 bar. The experimental results shown in

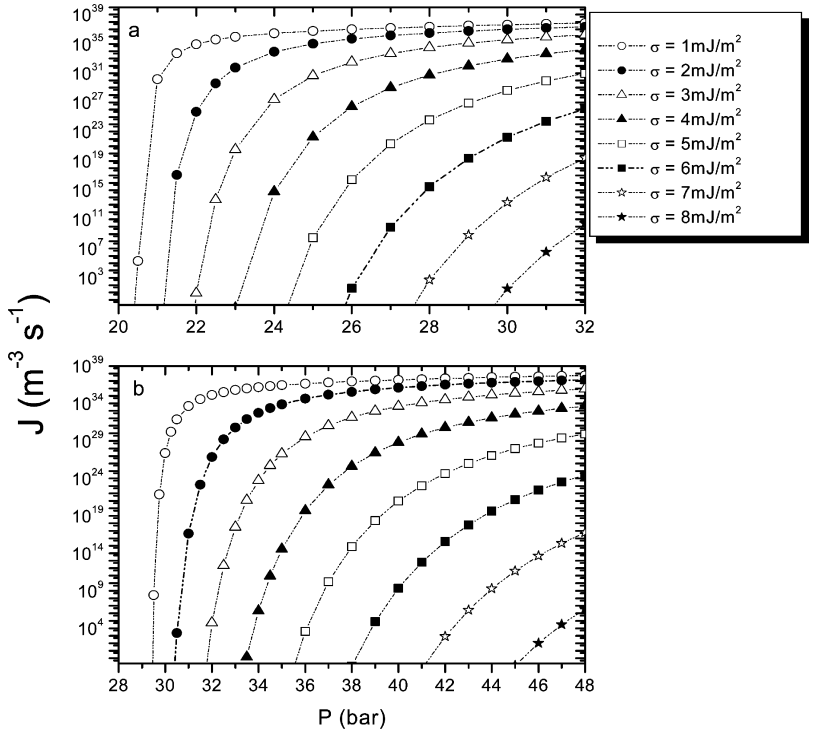

Figure 3. Comparison of the nucleation rate vs pressure with different surface energies specified (1−8 mJ/m^2) for CO_2 hydrate at the temperatures of (a) 276 and (b) 279 K.

dx.doi.org/10.1021/jp3021613 | J. Phys. Chem. B 2012, 116, 7296−7301

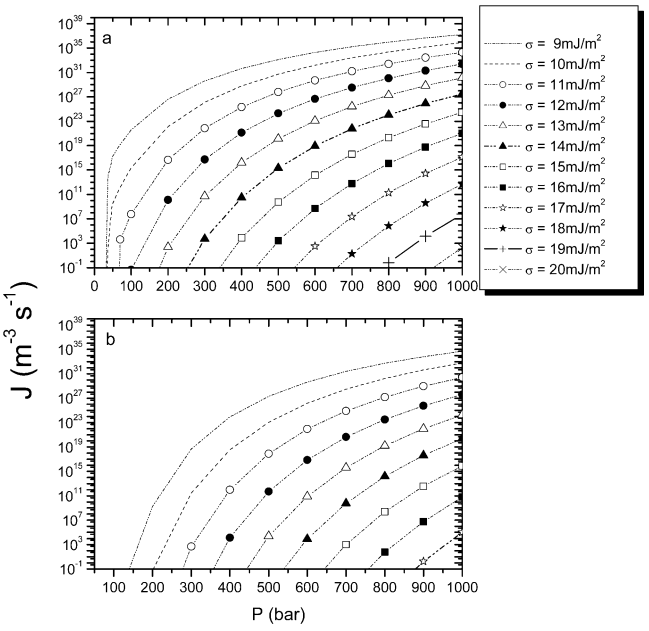

Figure 4. Comparison of the nucleation rate vs pressure with different surface energies specified (9−20 mJ/m^2) for CO_2 hydrate at the temperatures of (a) 276 and (b) 279 K.

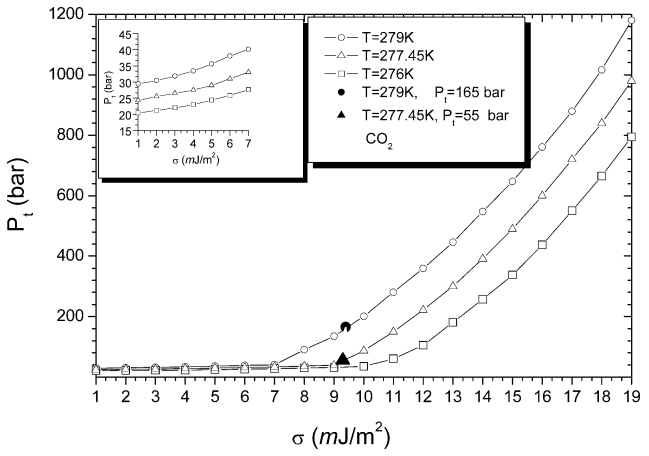

Figure 5. Threshold pressure (P_t) for CO_2 hydrate formation as a function of surface energy at the temperatures of 276, 277.45, and 279 K. The insert shows the same plot but with the small value of the surface energy ranging from 1 to 7 mJ/m^2. The arrow indicates those experimental ranges of pressure and temperature for stable CO_2 hydrate formation.[35]

Figure 6 are extracted from Figure 3 in the reference.[35] The experimental results indicate that at the temperature range of 277.45−278.85 K, stable CO_2 hydrates are formed between the pressure of 55 and 165 bar. We match those experimental ranges of pressure and temperature in Figure 5 and indicate it by the arrow. The comparison between the model prediction and the experiments performed by North et al.[35] suggests a surface energy of around 9.3 mJ/m^2. This value is very close to the recently reported hydrate/water interfacial energy of 7.5 ± 1.4 mJ/m^2 from molecular simulation.[28] In Figure 5 of the reference,[11] Kashchiev et al. showed an even smaller effective surface energy of around 2.7 mJ/m^2 for the experimental data for cyclopropane hydrate in aqueous solution. Estimations of the surface tension of clathrates from the Gibbs−Thomson equation in experiments at a maximum pressure of 414 bar[27]

Table 1. Threshold Pressure, P_t, Necessary for CO_2 Hydrate Formation with Different Surface Energies at 276, 277.45, and 279 K

σ (mJ/m^2)	T = 276K P_t (bar)	T = 277.45K P_t (bar)	T = 279K P_t (bar)
1	20.42	24.30	29.41
2	21.17	25.50	30.41
3	21.96	26.50	31.82
4	23.00	27.50	33.45
5	24.38	29.00	35.60
6	25.84	31.00	38.05
7	27.62	33.00	41.16
8	29.67	36.00	45.00
9	31.37	39.00	135
10	34.64	87.00	201
11	60	150	280
12	105	222	359
13	181	300	446
14	257	391	547
15	337	490	647
16	437	600	761
17	550	720	879
18	665	840	1016
19	794	980	1180

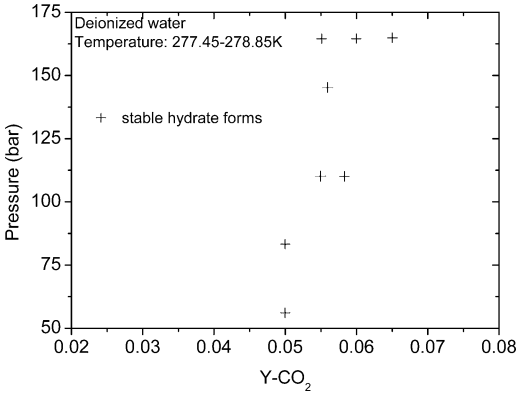

Figure 6. Experimental results for stable CO_2 hydrate formation at the temperature range of 277.45−278.85 K and the indicated pressures of 55−165 bar.[35]

and simulations at a pressure of 500 bar[36] render surface energy values between 28 to 36 mJ/m^2. For those high values of surface energy, hydrate formation requires extreme high pressure, which is hard to reach.

Figure 7 shows the comparison of the induction time versus driving force for CO_2 hydrate between the experimental data and the theoretical model. In the theoretical model, the method suggested in this work, eq 18, is used to fit the induction time measured from experiments over a range of supersaturation.[30] It should be noted that the pre-existing experimental results of the induction time were presented in terms of, $f_g/f_{eq} - 1$, where f_g is the fugacity at conditions studied, f_{eq} is the equilibrium fugacity at the temperature of experimental condition and Δg is the supersaturation. To facilitate the comparison, the theoretical results are presented in the same way. As it is seen, the induction time decreases with increasing driving force. The theoretical prediction matches reasonably with the experimental data. The experimental data for 276 and 279 K are scattered and there is no sufficient experimental data on such a system available to compare with the theoretical

dx.doi.org/10.1021/jp3021613 | J. Phys. Chem. B 2012, 116, 7296−7301

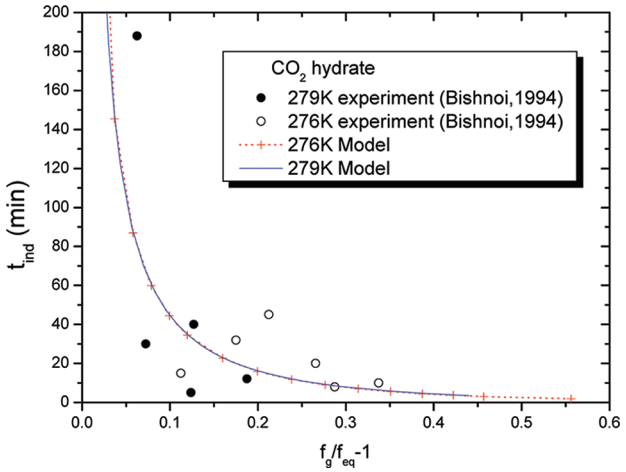

Figure 7. Comparison of the induction time vs driving force for CO_2 hydrate between the experimental data and the theoretical model.

prediction, to the best of our knowledge. In our fitting to the experimental data with eq 18, we avoid the surface tension but adjust the only unknown quantity, the average crystallite volume, $\bar{V}_c$, of the CO_2 hydrate, defined in eq 17. We derive a value of 0.238 mm^3 for the average crystallite volume for CO_2 hydrate. It provides insight for experimental study on hydrate nucleation and crystal growth even if the surface energy is unknown.

4. CONCLUSIONS

The hydrate formation kinetics was modeled based on the recent work of Kashchiev et al.[9−11] and Anklam et al.[29] The model was applied to CO_2 hydrate. The factors affecting the nucleus size, nucleation work, and nucleation rate were discussed. It is demonstrated that there is a strong dependence of the nucleation rate on the surface energy. Comparison of our results with the experimental data for stable CO_2 hydrate formation at the temperature range of 277.45−278.85 K and at pressure of 55−165 bar shows that the value of the surface energy between the CO_2 hydrate clusters and the aqueous phase is around 9.3 mJ/m^2, which is very close to the recently reported value of 7.5 ± 1.4 mJ/m^2 from molecular simulation. The threshold pressure is less sensitive to the temperature if the surface energy is not larger than 7 mJ/m^2. However, the threshold pressure is very sensitive to the temperature and increases significantly with the surface energy if it is over 7, 9, and 10 mJ/m^2 for the temperatures of 279, 277.45, and 276 K respectively. A theoretical method for computing induction time was suggested in this work, which avoids the surface energy and allows for fitting the theoretical prediction to the experimental data by adjusting the averaged crystallite volume, and we derive a value of 0.238 mm^3 for the average crystallite volume for CO_2 hydrate. This method can provide guide for experimental study on hydrate nucleation and crystal growth.

AUTHOR INFORMATION

Corresponding Author

*E-mail: Junfang.Zhang@csiro.au.

Notes

The authors declare no competing financial interest.

ACKNOWLEDGMENTS

Authors thank CSIRO Service Desk for providing Mathematica software.

REFERENCES

(1) Sloan, E. D. *Ind. Eng. Chem. Res.* **2000**, *39*, 3123.
(2) Klapproth, A.; Goreshnik, E.; Staykova, D.; Klein, H.; Kuhs, W. F. *Can. J. Phys.* **2003**, *81*, 503.
(3) Thompson, H.; Soper, A. K.; Buchanan, P.; Aldiwan, N.; Creek, J. L.; Koh, C. A. *J. Chem. Phys.* **2006**, 124.
(4) Cruickshank, M. J.; Masutani, S. M. *Sea Technology* **1999**, *40*, 69.
(5) Hammerschmidt, E. G. *Ind. Eng. Chem.* **1934**, *26*, 851.
(6) Chen, G. J.; Guo, T. M. *Chem. Eng. J.* **1998**, *71*, 145.
(7) Englezos, P.; Kalogerakis, N.; Dholabhai, P. D.; Bishnoi, P. R. *Chem. Eng. Sci.* **1987**, *42*, 2647.
(8) Englezos, P.; Kalogerakis, N.; Dholabhai, P. D.; Bishnoi, P. R. *Chem. Eng. Sci.* **1987**, *42*, 2659.
(9) Kashchiev, D.; Firoozabadi, A. *J. Cryst. Growth* **2002**, *243*, 476.
(10) Kashchiev, D.; Firoozabadi, A. *J. Cryst. Growth* **2002**, *241*, 220.
(11) Kashchiev, D.; Firoozabadi, A. *J. Cryst. Growth* **2003**, *250*, 499.
(12) Vysniauskas, A.; Bishnoi, P. R. *Chem. Eng. Sci.* **1983**, *38*, 1061.
(13) Vysniauskas, A.; Bishnoi, P. R. *Chem. Eng. Sci.* **1985**, *40*, 299.
(14) Zhang, J.; Hawtin, R. W.; Yang, Y.; Nakagava, E.; Rivero, M.; Choi, S. K.; Rodger, P. M. *J. Phys. Chem. B* **2008**, *112*, 10608.
(15) Zhang, J.; Guo, Y.; Yang, Y.; Kozielski, K. *J. Phys. B* **2009**, 42.
(16) Zhang, J.; Pan, Z. *J. Petrol. Sci. Eng.* **2011**, *76*, 148.
(17) Ohno, H.; Susilo, R.; Gordienko, R.; Ripmeester, J.; Walker, V. K. *Chem.—Eur. J.* **2010**, *16*, 10409.
(18) Zeng, H.; Moudrakovski, I. L.; Ripmeester, J. A.; Walker, V. K. *AIChE J.* **2006**, *52*, 3304.
(19) Zeng, H.; Wilson, L. D.; Walker, V. K.; Ripmeester, J. A. *J. Am. Chem. Soc.* **2006**, *128*, 2844.
(20) Mason, B. J. *The Physics of Clouds*; Clarendon: Oxford, 1971.
(21) Dufour, L.; Defay, R. *Thermodynamics of Clouds*; Academic: New York, 1963.
(22) Ben Clennell, M.; Hovland, M.; Booth, J. S.; Henry, P.; Winters, W. J. *J. Geophys. Res., [Solid Earth]* **1999**, *104*, 22985.
(23) Zhang, W.; Wilder, J. W.; Smith, D. H. *Aiche Journal* **2002**, *48*, 2324.
(24) Klauda, J. B.; Sandler, S. I. *Ind. Eng. Chem. Res.* **2001**, *40*, 4197.
(25) Henry, P.; Thomas, M.; Ben Clennell, M. *J. Geophys. Res., [Solid Earth]* **1999**, *104*, 23005.
(26) Uchida, T.; Ebinuma, T.; Takeya, S.; Nagao, J.; Narita, H. *J. Phys. Chem. B* **2002**, *106*, 820.
(27) Anderson, R.; Llamedo, M.; Tohidi, B.; Burgass, R. W. *J. Phys. Chem. B* **2003**, *107*, 3507.
(28) Sakamaki, R.; Yasuoka, K.; Ohmura, R.; Grzelak, E.; Wu, D. T.; Sum, K. Calculation of interfacial tensions between hydrate and liquid phases using molecular simulation. In *The 7th International Conference on Gas Hydrate (ICGH)*; Edinburgh: Scotland, UK, 2011.
(29) Anklam, M. R.; Firoozabadi, A. *J. Chem. Phys.* **2004**, *121*, 11867.
(30) Bishnoi, P. R.; Natarajan, V.; Kalogerakis, N. *International Conference on Natural Gas Hydrates* **1994**, *715*, 311.
(31) Soave, G. *Chem. Eng. Sci.* **1972**, *27*, 1197.
(32) Kashchiev, D. *Nucleation: Basic Theory with Applications*; Butterworth-Heinemann: Oxford, 2000.
(33) Sarshar, M.; Esmaeilzadeh, F.; Fathikalajahi, J. *Theoretical Foundations of Chemical Engineering* **2010**, *44*, 201.
(34) Jensen, L.; Thomsen, K.; von Solms, N. *Chem. Eng. Sci.* **2008**, *63*, 3069.
(35) North, W. J.; Blackwell, V. R.; Morgan, J. J. *Environ. Sci. Technol.* **1998**, *32*, 676.
(36) Jacobson, L. C.; Molinero, V. *J. Am. Chem. Soc.* **2011**, *133*, 6458.